The North African Journal of Scientific Publishing (NAJSP)
مجلة شمال إفريقيا للنشر العلمي (NAJSP)
E-ISSN: 2959-4820
Volume 3, Issue 3, 2025
Page No: 326-334
Website: https://najsp.com/index.php/home/index
SJIFactor 2024: 5.49 **0.71 :2024 (AIF) معامل التأثير العربي** **ISI 2024: 0.696**

A Bayesian Denoising Framework with a Joint Local/Non-Local Prior Distribution

Suad Ali Farag Hamoudah*
Department of Information Technology, Faculty of Humanities and Applied Sciences, Benghazi University, Tocra, Libya

إطار عمل بايزي لإزالة الضوضاء باستخدام توزيع قبلي مشترك محلي وغير محلي

سعاد علي فرج حمودة*
قسم تقنية المعلومات، كلية العلوم الإنسانية والتطبيقية، جامعة بنغازي، توكرة، ليبيا

*Corresponding author: suad.imbarak@uob.edu.ly

Received: July 20, 2025	Accepted: September 08, 2025	Published: September 11, 2025

Abstract:
This paper introduces a robust Bayesian framework for image denoising, designed to address the limitations of traditional local regularization methods. The approach is centered on a novel Joint Probabilistic Prior that synergistically integrates a local Markov Random Field (MRF) prior, which enforces smoothness, with a non-local prior derived from the Non-Local Means (NLM) principle, which preserves structural integrity. By combining these two complementary forces within a single energy function, the model can effectively suppress White Gaussian Noise while simultaneously preserving sharp edges and fine-grained textures. The optimal denoised image is estimated by minimizing the posterior energy function using a Maximum a Posteriori (MAP) approach, solved efficiently via a gradient descent algorithm. We conduct a comprehensive comparative analysis, evaluating our model against both a conventional MRF-only Bayesian model and the state-of-the-art BM3D algorithm across a wide spectrum of noise levels (σ=10 to 80). The results are conclusive: the proposed Joint Prior Model consistently and overwhelmingly outperforms the MRF-only, achieving, for instance, a remarkable +10.47 dB gain in PSNR at σ=60. Furthermore, the proposed model demonstrates highly competitive performance against BM3D, particularly in high-noise levels, validating the efficacy and robustness of the proposed framework. These findings establish the joint prior approach as a powerful and principled solution for high-fidelity image denoising.

Keywords: Image Denoising, Bayesian Inference, Joint Prior Model, Non-Local Prior, Markov Random Field (MRF).

الملخص
يقدّم هذا البحث إطارًا بايزيًا متينًا لمعالجة ضوضاء الصور، صُمّم لمعالجة أوجه القصور الكامنة في أساليب التنظيم المحلي التقليدية. يرتكز النهج المقترح على احتمال قبلي مشترك يدمج بشكل تكاملي بين، الاحتمال القبلي المحلي المبني على الحقول العشوائية الماركوفية(MRF) ، والذي يفرض درجة من النعومة، والاحتمال القبلي غير المحلي المشتق من مبدأ الوسائل غير المحلية(NLM) ، والذي يحافظ على البنية الهيكلية للصورة. ومن خلال الجمع بين هذين العاملين المتكاملين ضمن دالة طاقة واحدة، يصبح بالإمكان كبح الضوضاء الغاوسية البيضاء، بفاعلية، مع الحفاظ في الوقت ذاته على الحواف الحادة والتفاصيل الدقيقة للصور. يتم تقدير الصورة المنقّاة من الضوضاء عن طريق تقليل دالة طاقة الاحتمال الخلفي باستخدام مقاربة الاحتمال الخلفي الأعظم والتي تُحل بكفاءة عبر خوارزمية الانحدار التدرّجي. لقد أجرينا تحليلًا مقارنًا شاملًا، حيث تم تقييم النموذج المقترح مقابل كل من نموذج بايزي قائم على MRF فقط، وخوارزمية المطابقة القطاعية

والترشيح الثلاثي الأبعاد المتقدمة، وذلك عبر نطاق واسع من مستويات الضوضاء (σ=10 إلى 80) .وجاءت النتائج حاسمة، فقد تفوّق النموذج المشترك المقترح باستمرار وبفارق كبير على نموذج MRF فقط، محققًا على سبيل المثال مكسبًا ملحوظًا قدره 10.47+ديسيبل في قيمة PSNR عند σ=60. علاوة على ذلك، أظهر النموذج المقترح أداءً تنافسيًا للغاية مقارنة بالمطابقة القطاعية والترشيح ثلاثي الأبعاد، وخصوصًا عند مستويات الضوضاء العالية، مما يؤكد فعالية ومتانة الإطار المقترح. وتُرسّخ هذه النتائج مكانة النهج الاحتمالي القبلي المشترك كحل قوي وذو أسس منهجية لمعالجة ضوضاء الصور بدقة عالية.

الكلمات المفتاحية :تنقية الصور من الضوضاء، الاستدلال البايزي، النموذج القبلي المشترك، الاحتمال القبلي غير المحلي، حقل ماركوف العشوائي.

Introduction

Image denoising has long been recognized as a fundamental problem in image processing, aiming to reconstruct high-quality images from data corrupted by noise during acquisition, transmission, or storage. Such noise not only reduces the visual quality of images but also negatively impacts subsequent tasks such as analysis and recognition [1]. Early solutions relied on local filtering methods such as Gaussian smoothing and median filtering. Although computationally efficient, these methods often introduced undesirable artifacts, including edge blurring and the loss of fine structural details as in [2-4]. A significant methodological shift was introduced with Bayesian inference frameworks, which provided a probabilistic foundation for image restoration by modeling the posterior distribution of the clean image given its noisy observation. This paradigm was pioneered by [5], and later refined through the contributions of [6] and [7,8], subsequently extended its application to broader Bayesian modeling contexts, as reviewed by [9]. In parallel, Markov Random Fields (MRFs) emerged as effective priors for enforcing spatial smoothness while preserving discontinuities where necessary [10-16].

Another breakthrough came with the introduction of the Non-Local Means (NLM) filter, which exploited self-similarity across the image to preserve textures and repeated patterns more effectively than local approaches [17]. Complementing this, the bilateral filter. provided edge-preserving smoothing and became widely adopted as a post-processing tool. Subsequent research explored hybrid approaches combining Bayesian inference, MRFs, and NLM priors, supported by adaptive weighting strategies to balance smoothness with detail preservation using local statistical measures [18].

Meanwhile, the BM3D algorithm, established itself as a strong benchmark for classical denoising performance. More recently, despite the success of deep learning, classical model-based techniques remain highly relevant due to their interpretability, robustness, and lower computational demands. Building on this rich history, this work proposes a unified Bayesian framework that integrates MRF and NLM priors. We introduce a carefully tuned weighting scheme to create a joint prior that robustly suppresses noise without compromising perceptual fidelity. The proposed method is evaluated using the Peak Signal-to-Noise Ratio (PSNR), Structural Similarity Index (SSIM), Root Mean Square Error (RMSE), and is benchmarked against BM3D, demonstrating competitive performance and strong edge preservation across various Gaussian noise levels.

Material and methods

Image denoising within a Bayesian framework aims to estimate the true, clean image from its noisy observation by maximizing the posterior probability. This approach provides a robust statistical foundation for incorporating prior knowledge about image properties. The proposed method leverages this framework by combining complementary prior models to achieve superior denoising performance.

We consider the common scenario where a clean image, denoted as x, is corrupted by additive white Gaussian noise (AWGN) to produce an observed noisy image y. The degradation process can be modeled as the following equation:

$$y = x + n \tag{1}$$

where n represents the additive Gaussian noise, assumed to be independent and identically distributed (i.i.d.) with zero mean and variance σ_n^2, *i.e.,* $\boldsymbol{n} \sim \mathcal{N}(0, \sigma_n^2 \boldsymbol{I})$.

Bayesian Inference and MAP Estimation

According to Bayes' theorem, the posterior probability of the clean image x given the noisy observation y is proportional to the product of the likelihood function $p(y|x)$ and the prior probability $p(x)$ of the image:

$$p(x|y) \propto p(y|x)p(x) \tag{2}$$

The objective is to find the Maximum a Posteriori (MAP) estimate $\hat{x}$ of the clean image, which maximizes the posterior probability:

$$\hat{x} = \arg\max_{x} p(x|y) \tag{3}$$

By taking the negative logarithm of the posterior probability, the maximization problem in Eq(3) can be transformed into a minimization problem of an energy function:

$$\hat{x} = \arg\min_{x} \{-\log p(y|x) - \log p(x)\} \tag{4}$$

Notice that Eq (4) decomposes the problem into two main terms: the data fidelity term derived from the likelihood $p(y|x)$ and the regularization term derived from the prior $p(x)$.

The likelihood function $p(y|x)$ quantifies the probability of observing the noisy image y given a clean image x. Assuming AWGN, the likelihood follows a Gaussian distribution expressed as:

$$p(y|x) = \left(\frac{1}{2\pi\sigma_n^2}\right)^{N/2} \exp\left(-\frac{1}{2\sigma_n^2}\|y - x\|^2\right) \tag{5}$$

where N is the total number of pixels in the image. Taking the negative logarithm of Eq (5) yields the data fidelity term:

$$\begin{aligned} -\log p(y|x) &= \frac{1}{2\sigma^2}\|y - x\|^2 + \text{const} \\ E_{data}(\mathbf{x}, \mathbf{y}) &= \frac{1}{2\sigma_n^2}\|\mathbf{y} - \mathbf{x}\|^2 \end{aligned} \tag{6}$$

The prior probability $p(x)$ encodes our a priori knowledge about the statistical properties of natural images. The framework utilizes a novel joint prior combining local and non-local regularization. The MRF prior model local spatial dependencies, encouraging smoothness in homogeneous regions while preserving discontinuities. It is typically formulated as a Gibbs distribution:

$$p_{\text{MRF}}(x) = \frac{1}{Z}\exp\left(-\alpha \sum_{(i,j)\in\mathcal{N}} \phi(x_i, x_j)\right) \tag{7}$$

where Z is a normalization constant, α controls the prior strength, and ϕ is a potential function penalizing differences between neighboring pixels x_i and x_j. Usually, the quadratic potential is a common choice:

$$\phi(x_i, x_j) = (x_i - x_j)^2$$

leading to the energy term:

$$E_{\text{MRF}}(x) = \lambda_{\text{MRF}} \sum_{(i,j)\in\mathcal{N}} (x_i - x_j)^2 \tag{8}$$

where λ_{MRF} is the regularization weight.

The Non-Local Means (NLM) prior leverages the inherent self-similarity of images and asserts that similar patches across the image should have similar pixel values [19]. It can be formulated as:

$$E_{\text{NLM}}(x) = \lambda_{\text{NLM}} \sum_{i} \sum_{j\in\mathcal{S}(i)} w_{ij}(x_i - x_j)^2 \tag{9}$$

where λ_{NLM} is the regularization weight, x_i is the pixel to be denoised, and x_j are pixels in patches similar to the patch centered at i. The weights w_{ij} quantify the similarity between patches centered at i and j in the noisy image, computed as:

$$w_{ij} = \frac{1}{Z_i} \exp\left(-\frac{\|P_i - P_j\|^2}{h^2}\right) \tag{10}$$

where P_i and P_j are patches centered at i and j, respectively, h is a filtering parameter, and Z_i is a normalization factor.
The proposed Joint Prior Model combines the MRF and NLM priors into a single regularization term:

$$E_{\text{Prior}}(x) = E_{\text{MRF}}(x) + E_{\text{NLM}}(x) \tag{11}$$

By combining the data fidelity term Eq (6) and the joint prior term Eq (12), the total energy function to be minimized for MAP estimation is:

$$E(x) = \frac{1}{2\sigma^2}\|y - x\|^2 + E_{\text{MRF}}(x) + E_{\text{NLM}}(x)$$
$$E_{total}(\mathbf{x}) = \frac{1}{2\sigma_n^2}\|\mathbf{y} - \mathbf{x}\|^2 + \lambda_{MRF}\sum_{(i,j)\in\mathcal{N}}(x_i - x_j)^2 + \lambda_{nlm}\sum_i\sum_{j\in\mathcal{N}_i} w_{ij}(x_i - x_j)^2 \tag{12}$$

To find the optimal $\hat{\mathbf{x}}_{MAP}$, we employ an iterative optimization algorithm. Specifically, the Expectation-Maximization (EM) [20] algorithm can be used to estimate both the latent clean image $\mathbf{x}$ and potentially unknown model parameters (e.g., noise variance or prior parameters). Within each M-step of the EM algorithm, or as a standalone optimization for a fixed set of parameters, an iterative gradient descent approach is utilized. Starting with an initial estimate (e.g., the noisy image $\mathbf{y}$), the image is updated iteratively by moving in the direction opposite to the gradient of the energy function, as commonly applied in Bayesian image restoration:

$$\mathbf{x}^{(k+1)} = \mathbf{x}^{(k)} - \alpha\nabla E_{total}(\mathbf{x}^{(k)})$$

Here, $\mathbf{x}^{(k)}$ is the current image estimate, α is the step size, and $\nabla E_{total}(\mathbf{x}^{(k)})$ is the gradient of the total energy function. This gradient guides the iterative updates, pushing pixels towards a state that minimizes the energy, thereby balancing fidelity to the noisy data with adherence to the combined prior knowledge. Each iteration refines the image, progressively reducing noise while preserving structural integrity. where α is the step size (learning rate) and ∇E_{total} is the gradient of the total energy function with respect to $\mathbf{x}$. The gradient combines the forces from the data fidelity term (pulling $\mathbf{x}$ towards $\mathbf{y}$) and the two prior terms (regularizing $\mathbf{x}$ based on local smoothness and non-local similarity).

Numerical Experiments

The approach was evaluated on a standard grayscale image dataset as illustrated in Figure 1, which is commonly used in image processing tasks. The image has 280×196 pixels, explicit dimensions, and data type float32, normalized to a range of 0 to 1. Multiple noisy test images (some displayed in Figure. 1) were created by synthetically adding eight different levels of additive Gaussian noise with varying noise standard deviation σ (from 10 to 80) to evaluate the robustness against noise. This controlled degradation simulates realistic perturbations and enables quantitative performance comparison. Minimization of the energy functions for both models was performed using an iterative gradient descent algorithm as described previously. All experiments were conducted using Python 3.8.3 with pertinent libraries: NumPy, OpenCV, scikit-image, and Pandas 1.3.3. The quality of denoising was comprehensively evaluated using multiple metrics, including PSNR, SSIM, VIF, and RMSE.

In convergence behavior, this iterative optimization process progresses over a fixed number of iterations (commonly set to 50). However, as demonstrated in the convergence curves in Figure 2, both the energy function and the PSNR metric stabilize much earlier, around 18 to 20 iterations. Beyond this point, further iterations provide minimal improvement in image quality, indicating convergence. The algorithm balances the need to remain faithful to the observed noisy data with enforcing prior knowledge, ensuring the restored image is visually plausible and clean according to the joint prior model. The success of the proposed Joint Prior model relies heavily on careful tuning of the regularization parameters λ_{mrf} and λ_{nlm}, to strike an optimal balance between noise reduction and detail preservation. Through extensive empirical experimentation, we adopted a deliberately imbalanced configuration with λ_{mrf} =0.15 and λ_{nlm}= 2.0. This strategic weighting imposes a clear hierarchy wherein the non-local NLM prior, responsible for preserving structural integrity, dominates the local MRF prior, encouraging smoothness. In areas of conflicting guidance, such as at sharp edges, the model explicitly prioritizes structure preservation over smoothing, effectively addressing the critical challenge of

reducing noise without compromising perceptual details, thereby enabling high-fidelity image reconstruction.

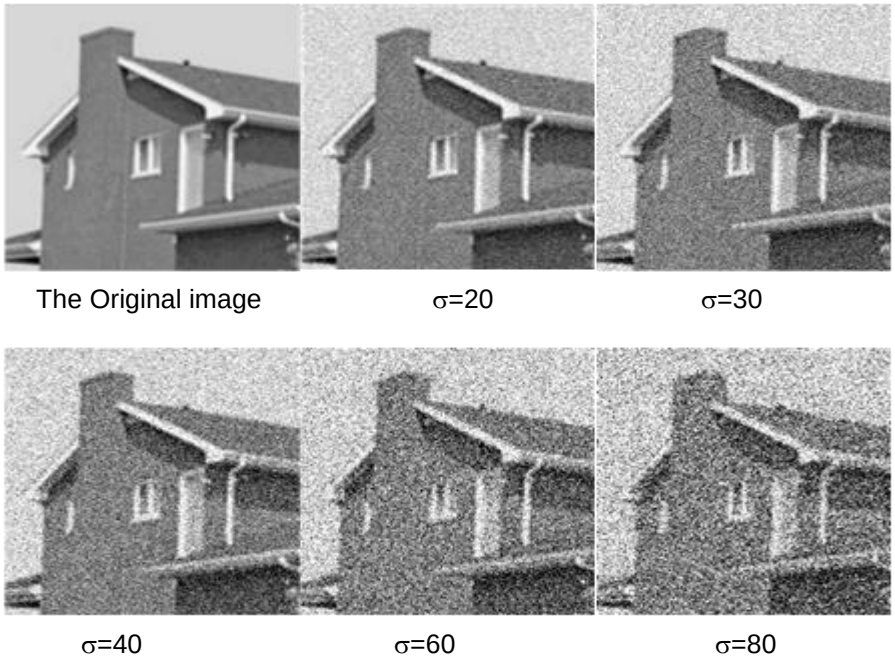

Figure 1: the original image and Gaussian noisy image for four levels (σ=20, σ=30, σ= 40, σ=60, σ=80)

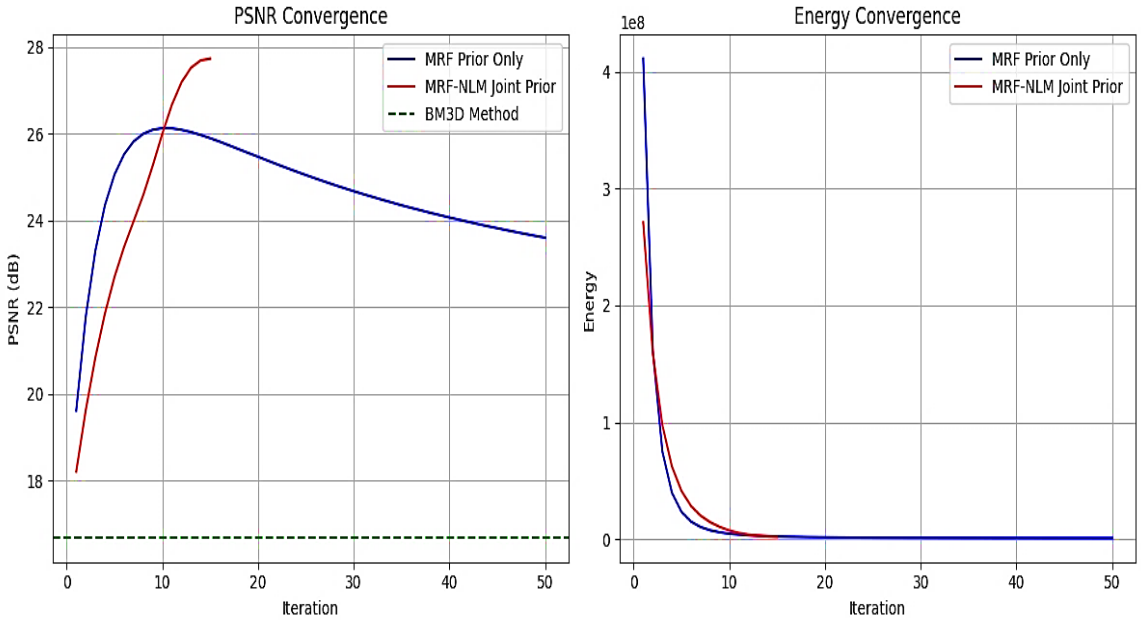

Figure 2: Convergence curves illustrating PSNR (left) and energy function (right) over iterations for baseline MRF and proposed joint MRF-NLM prior models.

Results and discussion

The results in Table 1. Demonstrate a significant superiority of the proposed Joint Prior Model over the baseline MRF method across all noise levels, confirming the effectiveness of combining local spatial consistency (MRF) with non-local similarity information (NLM). This integration allows the model to better exploit repeated structures, leading to superior noise suppression while preserving fine details. For instance, at σ = 20, the Joint Model achieves a PSNR of 32.94 dB (an 8.81 dB improvement over

MRF), a substantial SSIM increase from 0.42 to 0.89, and a VIF gain from 0.331 to 0.496, with RMSE significantly reduced from 15.48 to 5.74. Compared to BM3D as a criterion [21], the Joint Model delivers competitive results, often approaching BM3D's performance in PSNR and SSIM.

Table 1: Comparative Denoising Performance Across Various Noise Levels

Gaussian Noise ration	Method	PSNR (dB)↑	SSIM↑	VIF↑	RMSE↓
σ=10	Noisy	28.12	0.58	0.429	10.00
	MRF	30.01	0.67	0.442	8.68
	Joint Prior Model	33.80	0.92	0.548	5.20
	BMD3	38.07	0.95	0.649	3.31
σ=15	Noisy	24.61	0.51	0.337	14.99
	MRF	26.50	0.51	0.373	12.05
	Joint Prior Model	33.27	0.90	0.518	5.53
	BMD3	36.44	0.94	0.593	3.95
σ=20	Noisy	22.23	0.35	0.280	19.72
	MRF	24.13	0.42	0.331	15.48
	Joint Prior Model	32.94	0.89	0.496	5.74
	BMD3	35.26	0.92	0.550	4.49
σ=25	Noisy	20.35	0.28	0.240	24.47
	MRF	22.24	0.35	0. 267	19.69
	Joint Prior Model	32.50	0.89	0.483	6.04
	BMD3	34.21	0.91	0.522	5.09
σ=30	Noisy	18.84	0.24	0.207	29.13
	MRF	20.71	0.30	0.229	23.50
	Joint Prior Model	31.96	0.89	0.464	6.43
	BMD3	34.92	0.92	0.544	4.66
σ=40	Noisy	16.56	0.18	0.164	37.85
	MRF	18.46	0.23	0.182	30.46
	Joint Prior Model	30.53	0.88	0.413	7.58
	BMD3	31.41	0.89	0.440	6.98
σ=60	Noisy	13.49	0.12	0.113	53.95
	MRF	15.37	0.15	0.124	43.46
	Joint Prior Model	25.84	0.74	0.270	13.01
	BMD3	28.18	0.85	0.367	10.10
σ=80	Noisy	11.55	0.08	0.083	67,47
	MRF	13.40	0.11	0.091	54.51
	Joint Prior Model	20.63	0.44	0.151	23.72
	BMD3	25.02	0.81	0.300	14.50

For example, at σ = 25, the Joint Model achieves a PSNR of 32.50 dB versus 34.21 dB for BM3D, with nearly identical SSIM values (0.89 and 0.91 respectively). This highlights the model's ability to achieve a good balance between visual quality and computational simplicity. The robustness of the proposed approach becomes more evident with increasing noise levels. While all methods experience performance degradation with higher σ, the Joint Model exhibits a slower rate of decline compared to MRF. Even at σ = 40, it maintains a PSNR of 30.53 dB and an SSIM of 0.88, significantly higher than MRF's 18.46 dB and 0.23. At σ = 60, the Joint Model shows a PSNR of 25.84 dB (a +10.47 dB improvement over MRF) and an SSIM of 0.75, underscoring its ability to leverage non-local similarities even in severe noise.

Results at σ = 80 reveal the models' operational limits. While the MRF model becomes practically ineffective, the Joint Model still achieves a significant +7.23 dB PSNR improvement over the MRF baseline. However, its SSIM sharply drops to 0.45, indicating that extreme noise affects patch similarity measurements. BM3D shows greater resilience at this level (SSIM 0.81), suggesting its patch grouping strategy provides additional robustness. This gap highlights a promising direction for future research in developing more robust similarity metrics or integrating learning-based approaches to guide non-local search in highly corrupted images. The qualitative (visual) evaluations illustrated in Figures 3– 6 confirm the quantitative results presented in Figures 8 and 9, with the Joint Model producing visually cleaner images and better preserving fine details and edges compared to the MRF model, particularly in textured regions. This consistency between quantitative and qualitative analyses reinforces the proposed model's effectiveness and robustness across various noise levels.

(A) (B) (C)

Figure 3: Visual comparison of denoising results at Gaussian noise level (σ = 20) for (A) the MRF, the (B) proposed joint prior model, and (C the BMD3 method

(A) (B) (C)

Figure 4: Visual comparison of denoising results at Gaussian noise level (σ = 30) for(A) the MRF baseline, (B)the proposed joint prior model, and (C) the BMD3 method

(A) (B) (C)

Figure 5: Visual comparison of denoising results at Gaussian noise level (σ = 40) for (A) the MRF baseline, (B) the proposed joint prior model, and (C) the BMD3 method

(A) (B) (C)

Figure 6: Visual comparison of denoising results at Gaussian noise level (σ = 60) for(A) the MRF, (B) the proposed joint prior model, and(C) the BMD3 method

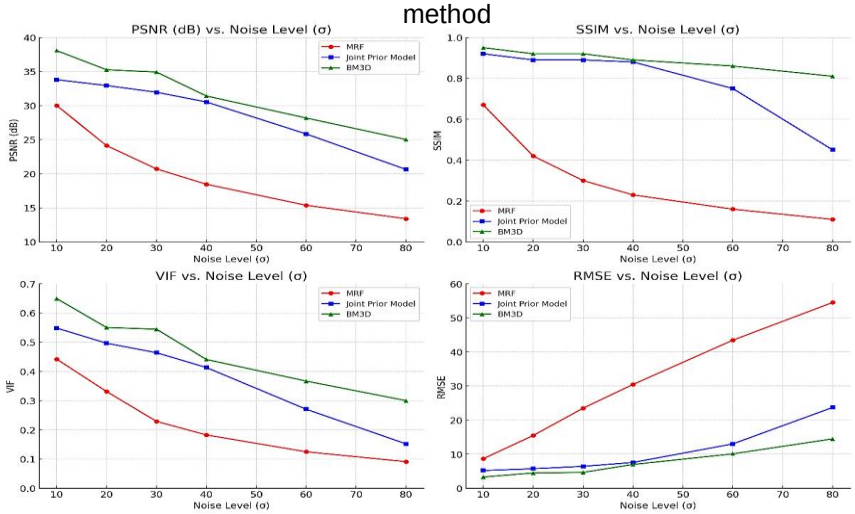

Figure 7: Variation of PSNR, SSIM, VIF, and RMSE values with noise standard deviation (σ) for the three evaluated methods.

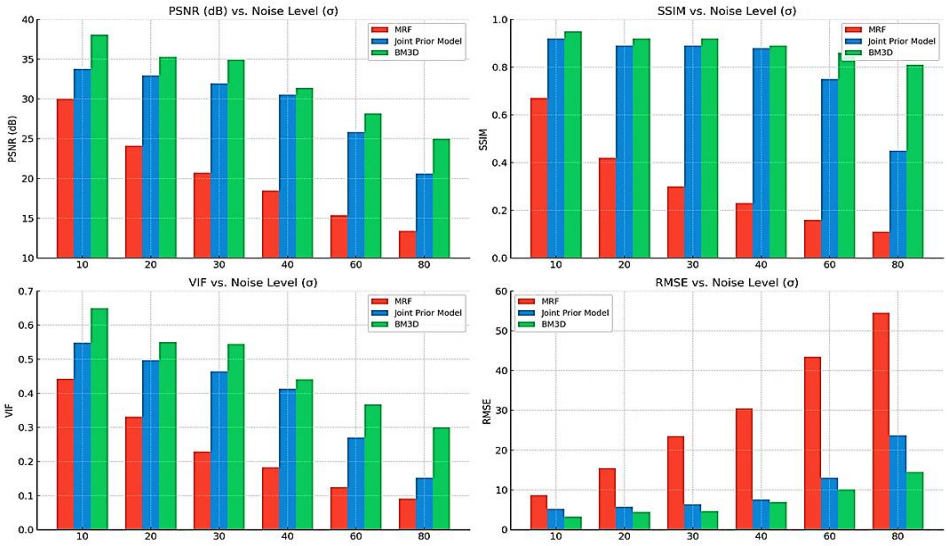

Figure 8: Comparison of PSNR, SSIM, and VIF at selected noise levels (σ = 10 to 80) for MRF, the proposed joint prior model, and BMD3.

Conclusions

This study at extreme noise levels solidifies the core thesis of this research. They unequivocally demonstrate that the local-only MRF prior is an inadequate model for all but the most trivial denoising tasks. The proposed Joint Prior Model, by integrating non-local information, provides a dramatic and robust improvement in performance. While its effectiveness begins to wane at the absolute limits of signal degradation (σ=80), its ability to function so effectively up to σ=60 and to still outperform the baseline so significantly at σ=80 validates it as a powerful and resilient framework. The performance gap between our model and BM3D at these extreme levels also clearly outlines a path for future research, focusing on enhancing the robustness of the non-local similarity search in highly noisy environments.

References

[1] B. R. Frieden, "Statistical models for the image restoration problem," *Computer Graphics and Image Processing*, vol. 12, no. 1, pp. 40–59, 1980.

[2] A. K. Jain, *Fundamentals of Digital Image Processing*. Englewood Cliffs, NJ, USA: Prentice-Hall, 1989.

[3] C. Tomasi and R. Manduchi, "Bilateral filtering for gray and color images," in *Proc. 6th Int. Conf. Comput. Vis. (ICCV)*, Jan. 1998, pp. 839–846.

[4] B. Desai, U. Kushwaha, and S. Jha, *Image Filtering Techniques: Algorithm and Applications*. Shirpur: SVKM's NMIMS Shirpur, 2020.

[5] S. Geman and D. Geman, "Stochastic relaxation, Gibbs distributions, and the Bayesian restoration of images," *IEEE Transactions on Pattern Analysis and Machine Intelligence*, vol. 6, no. 6, pp. 721–741, Nov. 1984.

[6] J. Besag, "Towards Bayesian image analysis," *Journal of Applied Statistics*, vol. 16, pp. 395–407, 1989.

[7] K. V. Mardia, "Bayesian image analysis," *Journal of Theoretical Medicine*, vol. 1, pp. 63–77, 1997.

[8] A. E. Gelfand, S. E. Hills, A. Racine-Poon, and A. F. M. Smith, "Illustration of Bayesian inference in normal data models using Gibbs sampling," *Journal of the American Statistical Association*, vol. 85, no. 412, pp. 972–985, 1990.

[9] K.-R. Koch, *Bayesian Image Restoration by Markov Chain Monte Carlo Methods*. Berlin, Germany: Springer, 2004.

[10] R. Kindermann and J. L. Snell, *Markov Random Fields and Their Applications*. Providence, RI, USA: American Mathematical Society, 1980.

[11] J. Besag, "On the statistical analysis of dirty pictures," *Journal of the Royal Statistical Society: Series B (Methodological)*, vol. 48, no. 3, pp. 259–302, 1986.

[12] R. G. Aykroyd and S. Zimeras, "Inhomogeneous prior models for image reconstruction," *Journal of the American Statistical Association*, vol. 94, pp. 934–946, 1999.

[13] S. Z. Li, *Markov Random Field Modeling in Image Analysis*. London, UK: Springer-Verlag, 2001.

[14] S. Roth and M. J. Black, "Fields of experts: A framework for learning image priors," in *Proc. IEEE Comput. Soc. Conf. Comput. Vis. Pattern Recognit. (CVPR)*, vol. 2, Jun. 2005, pp. 860–867.

[15] Y. Li et al., "A comprehensive review of Markov random field and conditional random field approaches in pathology image analysis," *Archives of Computational Methods in Engineering*, vol. 29, no. 8, pp. 1–31, 2020.

[16] B. Lee, J. Park, and Y. Kim, "Hidden Markov model based on logistic regression," Dept. of Statistics, Kyungpook Nat. Univ., Daegu, South Korea, 2023.

[17] A. Buades, B. Coll, and J. M. Morel, "A non-local algorithm for image denoising," in *IEEE Computer Society Conference on Computer Vision and Pattern Recognition (CVPR'05)*, vol. 2, 2005, pp. 60–65.

[18] M. Lebrun, A. Buades, and J. M. Morel, "A nonlocal Bayesian image denoising algorithm," *SIAM J. Imaging Sciences*, vol. 6, no. 3, pp. 1665–1688, 2013.

[19] S. Kindermann, S. Osher, and P. W. Jones, "Deblurring and denoising of images by nonlocal functionals," *SIAM J. Multiscale Modeling and Simulation*, vol. 4, no. 4, pp. 1091–1115, 2005.

[20] A. P. Dempster, N. M. Laird, and D. B. Rubin, "Maximum likelihood from incomplete data via the EM algorithm," *Journal of the Royal Statistical Society. Series B (Methodological)*, vol. 39, no. 1, pp. 1-38, 1977.

[21] K. Dabov, A. Foi, V. Katkovnik, and K. Egiazarian, "Image denoising by sparse 3-D transform-domain collaborative filtering," *IEEE Transactions on Image Processing*, vol. 16, no. 8, pp. 2080–2095, 2007.